Antennas and Metamaterials for Electromagnetic Energy Harvesting

by

Thamer Almoneef

A thesis
presented to the University of Waterloo
in fulfillment of the
thesis requirement for the degree of
Master of Applied Science
in
Electrical and Computer Engineering

Waterloo, Ontario, Canada, 2012

I hereby declare that I am the sole author of this thesis. This is a true copy of the thesis, including any required final revisions, as accepted by my examiners.

I understand that my thesis may be made electronically available to the public.

Abstract

The emergence of microwave energy harvesting systems, commonly referred to as rectenna or Wireless Power Transfer (WPT) systems, has enabled numerous applications in many areas since their primary goal is to recycle the ambient microwave energy. In such systems, microstrip antennas are used as the main source for collecting the electromagnetic energy.

In this work, a novel collector based on metamaterial particles, in what is known as a Split Ring Resonator (SRR), to harvest electromagnetic energy is presented. Such collectors are much smaller in size and more efficient than existing collectors (antennas). A feasibility study of SRRs to harvest electromagnetic energy is conducted using a full wave simulator (HFSS). To prove the concept, a 5.8 GHz SRR is designed and fabricated and then tested using a power source, an Infiniium oscilloscope and a commercially available patch antenna array. When excited by a plane wave with an H-field normal to the structure, a voltage build up of 611 mV is measured across a surface mount resistive load inserted in the gap of a single loop SRR. In addition, a new efficiency concept is introduced, taking into account the microwave-to-AC conversion efficiency which is missing from earlier work. Finally, a 9X9 SRR array is compared with a 2X2 patch antenna array, both placed in a fixed footprint. The simulation results show that the array of SRRs can harvest electromagnetic energy more efficiently and over a wider bandwidth range.

Acknowledgements

In the name of allah the most gracious, the most merciful:

First of all, I would like to thank God Almighty for providing me with the strength, health, patience and the tools to accomplish this thesis work.

Second, I would like to express my sincere gratitude to my supervisor, Prof. Omar Ramahi. I cannot thank him enough for his guidance and friendly assistance that helped me improve my technical skills and academic knowledge. Prof. Ramahi has been my inspiration as I hurdle all the difficulties and obstacles in the completion of this research work. I believe that having discussions with him is a peerless privilege.

I owe a debt of gratitude to my committee members Dr. Bo Cui and Dr. Karim Karim for serving in my examination committee and for their invaluable feedback. I greatly appreciate the time they devoted and their sincere advices. In addition, I would like to thank Dr. Dayan Ban for attending and participating in my seminar presentation and for his valuable feedback.

I would like to extend my utmost gratitude to my dear parents for their support, love and patience. Many thanks to my brothers and sisters for their advice, support and faithful love. I really apologize to all my family members for being away for a long period.

I am very lucky to be a member of an active and friendly research group. I would like to thank all my colleagues in the microwave and electromagnetics research group at the University of Waterloo: Dr. Muhammed Boybay, Dr. Babak Alavikia, Zhao Ren, Mohammed Alshareef, Ali Albishi, Ahmed Ashoor, Abdulaziz alqahtani, Abdulbaset Ali, Miguel Ruphuy, Ferhat Aydinoglu and special thanks to Dr. Mohammed M. Bait-Suwailam for his valuable support in regards to the fabrication process. Their hot discussions always sparked novel ideas.

This research was supported by the Saudi Arabian Ministry of Higher Education.

Dedication

To my parents

Table of Contents

List of Tables

List of Figures

Chapter 1

Introduction

1.1 Thesis Objective

The work presented in this thesis is aimed at harvesting electromagnetic energy. In the literature, this topic is presented as rectenna systems or Wireless Power Transfer (WPT) systems. Therefore, both systems should be reviewed and the differences between the two systems should be understood in order to contribute to this topic. Hence, there are three main objectives of this thesis:

- Review the history of microwave energy harvesting through the work presented in the literature under rectenna and WPT systems. *(Chapter 2)*
- Analyze the challenges, limitations and working mechanism of rectenna systems through simulation and fabrication. *(Chapter 3)*
- Propose new and novel structures (metamaterial particles) for collecting electromagnetic energy, which are smaller in size and more efficient than existing collectors (antennas). *(Chapter 4)*

1.2 Thesis Contribution

The research work presented in this thesis provides three main contributions: a novel collector based on metamaterial particles for harvesting electromagnetic energy is introduced. A proof of concept through simulation and measurement is provided. In addition, a new method for calculating the efficiency of collectors is proposed to account for the microwave-to-AC conversion efficiency which is missing from earlier work presented in the literature. Finally, a simulation study is conducted which compares an array of patch antennas and an array of metamaterial particles in terms of microwave-to-AC conversion efficiency, with arrays both occupying the same footprint.

1.3 Thesis Outline

The reminder of the thesis is organized as follows:

Chapter 2 reviews the history and development of Wireless Power Transfer (WPT) and rectenna systems. In addition, the working mechanism of WPT and rectenna systems are provided. This chapter also reviews the compromises and challenges one can face when designing a full rectenna system. Finally, the most common applications of rectenna systems and their working mechanisms are covered.

Chapter 3 provides detailed procedures for designing a full rectenna system operating at 2.45 GHz. The steps taken during the fabrication process are also listed. A microstrip-line fed patch antenna is then fabricated and its results were compared to the once obtained by simulation. A strong agreement is observed in the return loss plot. Finally, the rectifier circuit is fabricated and tested.

Chapter 4 proposes a novel and new energy collector based on metamaterials in what is known as a Split Ring Resonator (SRR). A brief overview of metamaterials and some of their applications is presented. Two validity tests are conducted through simulation to study the feasibility of using one type of SRRs to harvest electromagnetic energy. Then an experiment is conducted though testing and measurements; it yielded results that prove the concept of using SRRs as collectors. Finally, the efficiency of an array of 9 X 9 SRRs

is compared to that of an array of 2 X 2 patch antennas placed over an identical footprint. The SRR array resulted in at least 25% more efficiency and a wider bandwidth ,over which the energy is collected, than that of the antenna array.

Chapter 5 finally, reviews the main milestones presented in this thesis. In addition, some concluding remarks and suggestions for future work are provided.

Chapter 2

Background

2.1 Introduction

This chapter provides a comprehensive overview of the most important milestones in the history and development of WPT systems, from the work and experiments of Hertz up to the date of this thesis. In addition, the working mechanism of WPT and rectenna systems, and some existing design challenges are discussed. Finally, a number of promising applications of rectenna systems along with a brief description of their operating mechanism are presented.

2.2 Historical Milestones

2.2.1 Early History

The notion of Wireless Power Transfer (WPT) was sparked in 1888 when Heinrich Hertz demonstrated electromagnetic wave propagation in free space [13]. Hertz used half wavelength dipoles operating at 500 MHz along with parabolic reflectors for transmitting and receiving electromagnetic energy. The high frequency power was generated by charging the opposite halves of the dipoles with high voltage in order to develop an arc across the gap.

As a result energy is stored in the gap, forming oscillations, and then the half wavelength dipoles radiate some of the oscillating energy as microwaves [52]. Hertz's experimental work constitutes crucial validation of Maxwell's hypothesis in regards to electromagnetic propagation in free space.

At the turn of the 20th century, further experiments on the concept of wireless power transfer were conducted by Nickola Tesla. A grant of $30,000, offered by Colonel John Jacob Astor, was used to build a gigantic coil resonating at 150 kHz, which was then placed in a large building in Colorado Springs, Colorado. Over the coil, was raised a 60 m pole topped by a 1 m diameter copper ball. The coil was then excited with low frequency power of 300 kW obtained from the Colorado Springs' electric power company. Consequently, a large RF potential was produced on the sphere, reaching 100 MV. After all his hard work at the Colorado Springs laboratory, Tesla was able to light 200 light bulbs placed 42 km away from the base station [18]. Tesla's work intrigued many researchers in Japan [57] and the US [1];however, technological limitations prevented them from progressing in this area.

It was not until the 1950s that the WPT became a useful technology, with the development of high power microwave tubes by the Raytheon Company. These tubes were considered essential for transmitting efficient high power at GHz frequencies. In 1963, William C. Brown, a pioneer in the concept and development of WPT, and his colleagues, demonstrated the first complete and efficient WPT system to a group of United States Air Force officials who funded the high power microwave tubes. In the demonstration, DC power was first converted to microwaves at 2.45 GHz and a power level of 400 W. A horn antenna was used to transmit the generated microwave energy, illuminating a reflector, which then bounced back the energy to its focal point. At the focal point, a diagonal horn antenna was placed to collect the microwave energy, which was converted back to DC by means of thermionic diodes. Conversion efficiencies of only 50% were realized [52].

Due to the low AC to DC conversion efficiency, which is attributed mainly to the diode, researchers have since focused on developing new and more efficient diodes. As a result, Hewlett-Packard Associates offered their new silicon Schottky-barrier diodes to C. Brown's group [12]. This type, the 2900 diodes, has the following advantages: much greater efficiency, much smaller size, and better capability of handling power than any of the previous diodes.

Both the development of high power microwave tubes and of the silicon Schottky-barrier diodes represent a paradigm shift in the history and development of the WPT technology.

In 1975, another key experiment was conducted in the Mojave Desert at the Jet Propulsion Laboratory's (JPL) Goldstone Facility to show the feasibility of transferring microwave power over a long distance. In this experiment, a new record was reached in terms of the amount of power received and the total distance over which the power was transmitted. The setup of the experiment consisted of a high powered klystron, which created microwave energy at 2.388 GHz and then fed it to a 26-m transmitting parabolic antenna as shown in Figure 2.1 [52]. This antenna excited a 26 m^2 rectenna (rectifying antenna) array located 1.54 km away. The rectenna array contained 4590 rectenna elements arranged in 17 panels, each panel consisting of 270 rectennas. Each rectenna element utilized a dipole antenna 0.47λ in length for capturing the microwave energy. Every two adjacent dipole antennas were separated by 0.6λ to maximize the collected microwave energy [19]. A set of lights were used as loads, each rectenna panel devoted to powering two lights. The total DC power collected by the rectenna array was over 30 kW, representing a total conversion efficiency of 84%. Overall, the developed WPT system in the Goldstone experiment was deemed successful for its ability to transmit power over a long distance, to demonstrate high conversion efficiency and to survive various weather conditions.

It is of interest to note that in parallel to the work accomplished by the Americans in regards to WPT, Canadian and Japanese researchers have developed their own programs, which contributed significantly to the advancement of WPT. An example of such a program developed by Canadian researchers is the Stationary High Altitude Relay Program (SHARP) and for those conducted by the Japanese are the Microwave Ionosphere Nonlinear Interaction Experiment (MINIX) and the Microwave Lifted Airplane Experiment (MILAX). For brevity, those programs are only mentioned ; however, details of each program can be found in [46, 33, 24] respectively.

Since the total efficiency of the WPT system depends significantly on the receiving system, commonly referred to as the rectenna system, research on this subject has focused on developing various rectenna systems that yield higher conversion efficiencies. In 1977, W. C. Brown at Raytheon developed a 2.45 GHz rectenna system that reached a conversion efficiency of 90.6% [11]. Both the dipole antenna and the transmission lines used in this

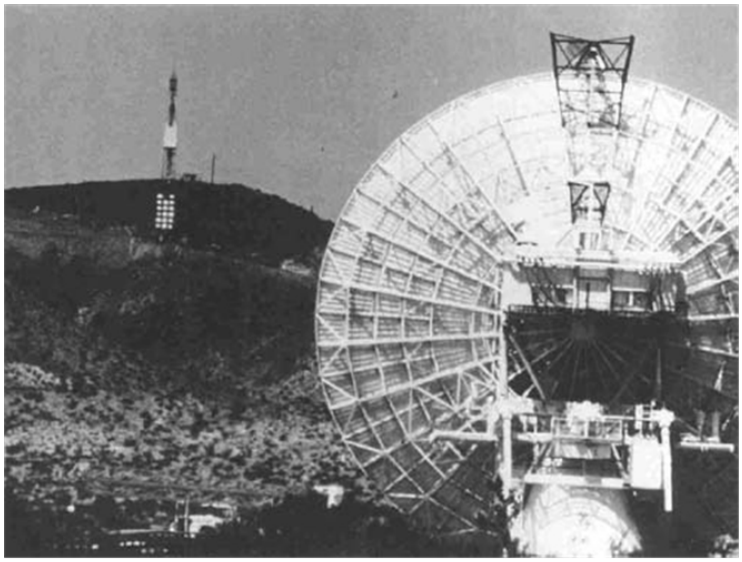

Figure 2.1: A picture showing the experiment conducted at the JPL Goldstone facility in the Mojave Desert.

system were made out of aluminum bars, and the microwave power collected by the antenna was converted to DC using a GaAs-Pt Schottky barrier diode. The conversion efficiency of this rectenna system is recognized as one of the greatest efficiencies ever recorded [34].

In 1985, Brown and Triner developed a revolutionary rectenna system using printed thin film technology. The rectenna system was designed to operate at 2.45 GHz and was able to achieve 85% conversion efficiency [14]. The main advantage of using such technology is its light weight, being 10 times lighter than previously developed rectennas. Since then, most rectenna systems have been made using photolithographic etching techniques for their ease of fabrication, low cost and light weight [52].

2.2.2 Recent Development

In most of the aforementioned experiments, rectenna systems have been designed to operate at around 2.45 GHz due to the limitations of the microwave energy sources available then. However, in 1991 a 35 GHz rectenna was developed by ARCO Power Technologies, with a

total conversion efficiency of 72% [30]. A low atmospheric absorption is the main advantage of operating in the vicinity of this frequency but doing so requires the use of more expensive and inefficient components [34].

In 1992, to compromise among efficiency, component cost and size, the first C band rectenna array was designed, operating at 5.87 GHz. The rectenna array was comprised of 1000 dipole antennas, which fed rectifier circuits with a silicon quad-bridge Schottky diode having a high reverse voltage. This new diode has the advantage of higher power-handling capabilities than those of the previously used GaAs diodes [10]. Conversion efficiencies exceeding 80% were obtained.

Up to that time, the main tools used to analyze and design rectennas were Libra [60], Touchstone [2], and Transmission Line Models [10]. It was not until 1997 that a full wave simulator was used by K. Chang's group at Texas A&M University to design a complete rectenna system. They have used I3ED by Zeland to iteratively design the length and width of the microstrip-lines of a dipole antenna, a low pass filter and the transmission lines linking them. A total RF-to-DC conversion efficiency of 82% was achieved with input power levels of 50 mW at 5.8 GHz [35]. After this point, most of the designs of rectenna systems have incorporated highly efficient full wave simulators such as HFSS, ADS, I3ED and CST. Using such advanced programs allows the designer to simulate both the antenna and the passive components simultaneously.

For the last decade, researchers have focused on improving different aspects of rectenna systems to suit the targeted applications. Such aspects include, but are not limited to:

- Antenna polarization (*i.e.,* linear/circular)
- Antenna type (*i.e.,* rectangular patch, bowtie, dipole, etc.)
- Operating frequency (*i.e.,* single/dual)
- Total size of the rectenna system
- Type of filter (*i.e.,* low-pass/band-pass)
- Impedance bandwidth

- Type of diode
- Rectifier circuit (*i.e.,* half-wave, full-wave, voltage doubler, etc.)
- Substrate material
- Feeding mechanism (*i.e.,* probe, micro-strip, aperture, etc.)

There is no absolute freedom in optimizing each aspect independently as a change in one aspect will alter one or more other aspects undesirably. Therefore, there is always a trade off when one or more aspects are optimized. Depending on the targeted application, one can balance those aspects to arrive at the desired rectenna performance.

Most of the recent microwave rectenna systems have been designed to operate in the range of frequencies between 1-35 GHz. Total conversion efficiencies of 50-80% are reachable when operating at frequencies in the C-band (*i.e.,* 5.8 GHz) as in [16, 50, 38]. However, the conversion efficiency degrades as the operating frequency increases, as in the case of rectennas working in the X-band [37] and the Ka-band [43], where efficiencies of only 21% and 35% are realized, respectively. Even though operating at higher frequencies exhibits a noticeable degradation in the total conversion efficiency, it has the advantage of miniaturizing the total size of the rectenna system, which is crucial for applications where portability is the primary concern. Hence, there is a trade off between efficiency and size when rectennas are designed at various frequencies.

Since the power availability is not always guaranteed when working at a narrow band of frequencies, operating at dual frequencies increases the reliability of rectenna systems. In such designs, rectennas utilize dual antennas that ,when designed properly, can receive the microwave energy at two ranges of frequencies (*i.e.,* 2.45 and 5.8 GHz) as in [42, 53, 27]. However, using dual-frequency rectennas increases the total size of the system due to the use of an additional antenna. A decrease in the total conversion efficiency is also noticeable since the matching network, the output load, and the diode input impedance must be optimized to maximize the power at both frequencies and, therefore, a compromise is always present between the two operating frequencies. Another practical way to increase the reliability of rectenna systems is by the use of wide band antennas. However, designing

a wide band matching network between the antenna and the microwave diode that always ensures maximum power transfer is somehow an intricate task due to the nonlinear behaviour of the diode, which has an input impedance that varies with the input power level and the operating frequency. Energy harvesting is an example of a rectenna application where power availability at the connected load or device is an important requirement.

Recent work on rectenna systems has incorporated Split Ring Resonators (SRRs) to miniaturize the size of the antenna, as in [61], and to suppress harmonics generated by the rectifier circuit, as in [25]. Ziolkowski and his group at the University of Arizona have designed an electrically small rectenna that operates at 1.5754 GHz, utilizing a metamaterial inspired structure. Using such a structure enables a dramatic reduction in the total size of the rectenna system while operating at lower frequencies, solving the problem faced in previous rectennas [62]. A detailed description of the working mechanism of SRRs and the feasibility of using them to harvest microwave energy is presented in Chapter 4.

2.3 Applications of Rectenna Systems

The advent of rectenna systems has greatly advanced many technologies that strive for energy, from powering an implantable artificial heart to tracking and identifying objects in security systems. Rectennas have countless potential applications since their primary goal is to deliver wireless DC power efficiently. Initially, rectennas were developed by Raytheon Company in response to the American Air Force requiring a device that could be attached to a helicopter and rectify microwave energy when a beam is pointed at the device. Brown and his colleagues developed a rectenna array that contains several thousands of point contact silicon diodes. The array produced a DC power level of approximately 200 W. As a result, the group were able to demonstrate a microwave-powered helicopter that can run for at least 10 hours continuously at an altitude of 28 meters above the transmitting antenna [12].

As a consequence of the success achieved in the helicopter demonstration, researchers showed a great interest in using rectennas to solve the global energy crisis by providing a clean and affordable energy source instead of using the harmful method of burning fossil

fuels. In 1968, Petter E. Glasser proposed a concept that uses rectennas to harvest energy from space in what is known by Space Solar Power (SSP). The working mechanism of the SSP concept can be understood by the following four main steps [22]:

1. Collect the solar energy from space and convert it to electricity;
2. Convert the collected power to microwaves and transmit it to Earth;
3. Receive the microwave energy and convert it back to electricity using large rectenna arrays;
4. Provide the collected energy to the power grid.

An example of rectenna array connected to the power grid is shown in Figure 2.2. The United States Department of Energy (DoE) and the National Aeronautics and Space Administration (NASA) has dedicated extensive research to examining the feasibility of such system. Results have shown a great promise for the future of energy. However, it could take decades before the SSP concept is implemented all over the world since it must outweighs the existing methods in terms of cost, reliability and sustainability.

Another vital application of rectenna systems that has excelled rapidly in the last decade is Radio Frequency Identification Systems (RFIDs). In an operational RFID system, there are two main components: a tag (transponder), which contains electronically stored data, and a reader (interrogator) that can read the stored data of the tag. First, the reader transmits RF energy to the tag; then the tag, which is attached to the object to be identified or tracked, receives the energy and sends back a coded signal to the reader. The reader then retrieves the data and responds accordingly (*i.e.,* activates an alarm) [18]. Here, the tag represents a rectenna system since it mainly consists of an antenna, a diode and a microchip. The tag can be either active or passive depending on the requirement of an internal power supply. An active tag, which requires a secondary source of energy in addition to the rectified microwaves, can read data in the range of between 20-100 meters from the interrogator. A passive tag, on the other hand, requires no internal source of energy and usually can respond to a reader at a shorter range than that of an active tag [58]. RFIDs are commonly used in industrial and commercial companies

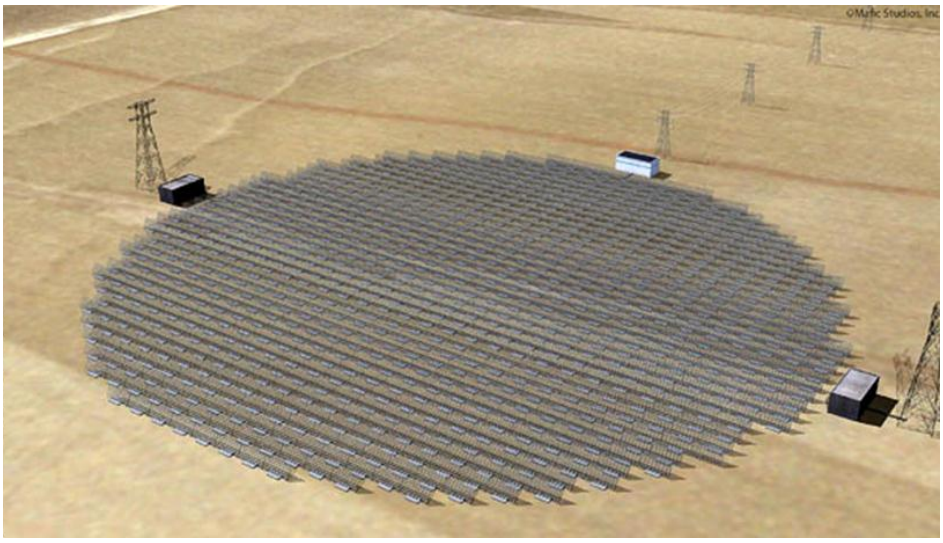

Figure 2.2: A schematic of a receiving rectenna array station connected to the grid. from:http://www.solarfeeds.com/powersat-a-new-space-solar-player/

as tracking and identifying tools for numerous objects, such as for tracking baggage in airports [3], surveillance and security systems [56], tracking pets or endangered animals [29], anti-collision systems [26], and even monitoring oil drill-pipes [51].

Other active research areas where rectennas find promising future applications include but are not limited to driving mechanical actuators at high voltages (50 V) [21], wireless power transfer to a sensor buried in concrete [48], and implantable rectennas for biotelemetry communications [28].

2.4 Operation of Rectenna Systems

A rectenna or a rectifying antenna is part of a larger system known as a wireless power transfer system (WPT). A common WPT system consists of three main subsystems: a transmitter, a travelling medium (*i.e.,* free space), and a receiver, as shown in Figure 2.3. The function of the first block, which represents a transmitter, is to convert DC power to

microwaves using a transmitting circuit and a transmitting antenna. These microwaves will radiate through the transmitting antenna and travel across free space towards a receiver represented by the third block. The receiver, which represents a rectenna system, converts the microwaves to AC power using a receiving antenna. Then the captured AC power is converted back to DC using a rectifying circuit. Hence, the name rectenna, which combines the words of the main components that comprise it. The total efficiency of the WPT system is the product of the transfer function of each functional block, which can be expressed as [40]:

$$\eta_o = \eta_t \times \eta_f \times \eta_r \tag{2.1}$$

where η_o represents the overall efficiency of the WPT system, η_f is the free space efficiency, and η_r denotes the total efficiency of the rectenna system. Usually in WPT systems, the transmitter efficiency η_t is assumed to be unity.

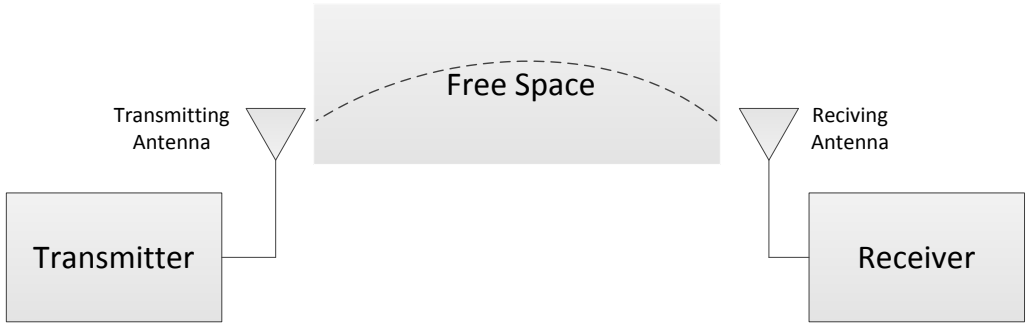

Figure 2.3: Functional blocks of a typical Wireless Power Transfer (WPT) system.

Zooming into the the third block, there are five main elements that form a rectenna system as shown in Figure 2.4. The electromagnetic energy is captured using a receiving antenna operating at the desired frequency. Then, an RF filter is used to transform the antenna impedance to that of the diode, reducing reflections caused by any impedance mismatch. The RF filter also suppresses the unwanted harmonics caused be the nonlinear

behaviour of the diode. After the AC power has channeled maximally from the antenna through the RF filter, a diode (*i.e.,* schottky diode) is used to rectify or convert the collected AC power to DC. To ensure that AC power does not reach the load, a DC filter is inserted after the diode which mainly consists of a shunt capacitor that acts as a short circuit for higher frequencies. Then, a resistive load is used to consume the DC power.

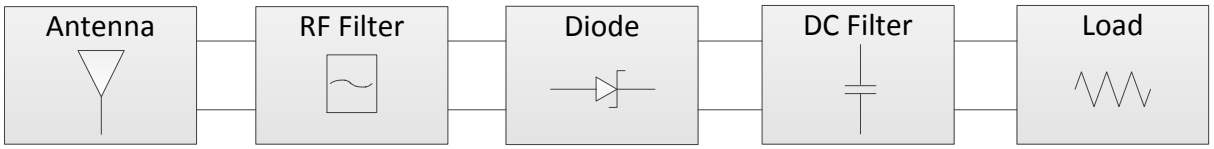

Figure 2.4: a block diagram for a generic rectenna system using an antenna as the primary collector.

The total efficiency of the rectenna system in most of the previously developed rectennas is obtained using the following relation [62]:

$$\eta_r = \frac{P_{out}}{P_{in}} \tag{2.2}$$

where the output power P_{out} and the input power P_{in} are given by:

$$P_{out} = \frac{{V_L}^2}{R_L} \tag{2.3}$$

$$P_{in} = \underbrace{G_r \left(\frac{\lambda^2}{4\pi}\right)}_{\text{Effective Area}} \times \underbrace{\left(\frac{G_t P_t}{4\pi D^2}\right)}_{\text{Incident Power Density}} \tag{2.4}$$

where V_L and R_L are the voltage across and the resistance of the connected load. In Eq. 2.4, G_t is the transmitter gain, P_t is the transmitted power and G_r is the gain of the receiver antenna. In measurements, the rectenna under test is usually placed a distance D away from the transmitter to ensure the far field condition is satisfied.

It is of interest to note that Eq. 2.2 represents the AC-to-DC conversion efficiency, which mainly depends on the type of diode used, the input power level and the optimal

resistive load. Hence, such equations do not take into account the efficiency of the collector (*i.e.,* antenna) where the microwave energy is converted to AC power in the first place. Therefore, a new method for computing the efficiency of rectenna systems is introduced in Chapter 4. In this method, the efficiency of the collector (microwave to AC link) is considered which is missing from earlier work.

Chapter 3

Design and Fabrication of 2.45 GHz Rectenna System

3.1 Introduction

This chapter presents the procedures for designing a full rectenna system operating at 2.45 GHz. First, a patch antenna fed by a microstrip line is designed and fabricated. Then a rectifier circuit consisting of a quarter wavelength transformer, a schottky diode, and an output filter is designed for an input impedance of 50 Ω to maximize energy transfer when attached to the patch antenna. Here, the primary goal of designing a rectenna system is not maximizing system efficiency but rather understanding the design procedures and the challenges one can face when building a rectenna system.

3.2 Microstrip Antenna

3.2.1 Theoretical Background

An antenna is one of the fundamental components in any rectenna system since it is the primary energy source that feeds the rectification circuit. Microstrip-type antennas are

widely used in communication systems due to their lightweight, low cost, ease of fabrication, low profile, conformability to planar and non-planer surfaces and mechanical robustness. However, microstrip antennas suffer from various drawbacks that limit their applications significantly such as narrow bandwidth, low power handling capability, high feed network losses and high cross polarization [23]. A great deal of research has been aimed at improving antenna characteristics and overcoming the aforementioned drawbacks of microstrip antennas. The advancements in recent antenna technology and the emergence of new concepts such as metamaterials have overcome most of these drawbacks or at least mitigated them to a certain extent. Therefore, antennas in the majority of rectenna systems if not all are of a microstrip type.

Microstrip antennas consist of a metallic layer, dielectric substrate, ground plane and feeding mechanism. Choosing the proper feeding configuration is important to achieve better impedance matching to the rectification circuit. The most common types, used in practise, are the coaxial probe, microstrip line, proximity coupling and aperture coupling [9]. Here, the microstrip line feeding mechanism is used since both the antenna and the rectification circuit can be easily fabricated in one plane. In addition, the microstrip line method is simple to match since the input impedance of the antenna can be varied by controlling the position and the width of the transmission line.

Recent rectenna research has focused on using circularly polarized (CP) microstrip antennas. Rectennas that utilize CP antennas have the advantage of constant output voltage, which is essential in applications where the connected load is rated at certain voltage levels. Furthermore, CP antennas can receive the incoming signal regardless of their position. This capability is particularly important in RFID tags where an interrogator can identify or track a certain tag irrespective of its orientation. A microstrip antenna by its nature is linearly polarized (LP) since it is designed to operate at a single mode. For an antenna to radiate circular polarized waves, two orthogonal modes must be excited, having equal magnitudes but with a 90° phase shift. This condition can be achieved by introducing some modifications to the antenna design. The common two methods to produce CP antennas are single and dual-orthogonal feeding mechanisms. CP can be obtained with a single feed by truncating the corners of a patch or by slightly perturbing some segments of the antenna as in Figure 3.1a. The main objective of these modifications is to disturb

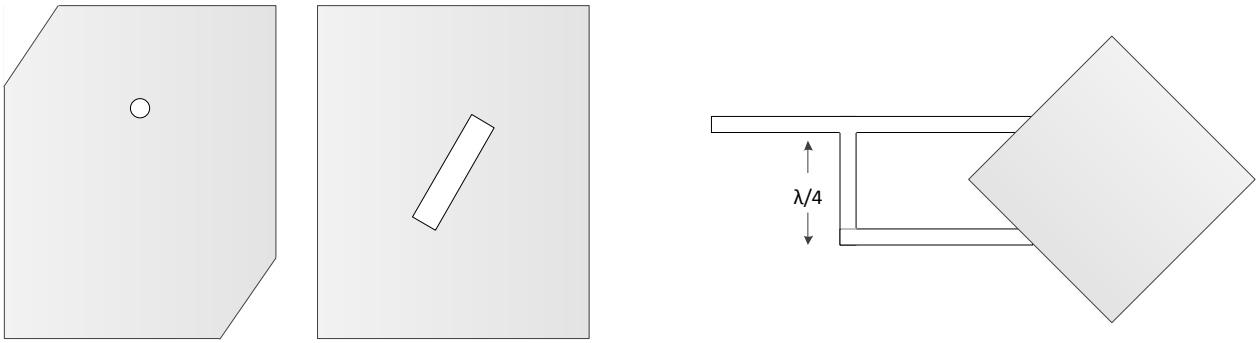

(a) Single fed circular polarized antennas.

(b) Dual fed circular polarized antenna.

Figure 3.1: Single and dual fed circular polarized antennas.

the current density in such a way that the two modes are excited. In the dual-orthogonal feeding method, the two modes are excited by employing an external power divider circuit as in Figure 3.1b. To understand the type of polarization of any antenna, a plot of Axial Ratio (AR) vs. Frequency is used. An AR of less than 3 dB is indicative of an antenna radiating circular polarized waves within a certain range of bandwidth. The transmitter and the receiver antennas must have the same polarization, to avoid polarization mismatch and to maximize the energy collected by the receiving antenna.

3.2.2 Antenna Design

Since the goal of the work presented in this chapter is to clarify the working mechanism of rectenna systems, the basic LP microstrip-line fed patch antenna is selected.

A patch antenna is a resonance-based structure having a resonance frequency that depends on the various dimensions of the antenna, as shown in Figure 3.2. The width W and the length L can be found using the following relation [9]:

$$W = \frac{\upsilon_\circ}{2f_r}\sqrt{\frac{2}{\epsilon_r + 1}} \tag{3.1}$$

$$L = \frac{\lambda}{2} - 2\Delta L, \tag{3.2}$$

where $\upsilon_\circ$ is the speed of light, ϵ_r is the dielectric constant, and f_r is the resonance frequency of the antenna. The extended incremental length ΔL due to the fringing effect can be found from

$$\Delta L = 0.412(h)\frac{(\epsilon_{reff} + 0.3)\left(\frac{W}{h} + 0.264\right)}{(\epsilon_{reff} - 0.258)\left(\frac{W}{h} + 0.8\right)} \tag{3.3}$$

where h is the height of the substrate, and the effective dielectric constant ϵ_{reff} is given by the following:

$$\epsilon_{reff} = \frac{(\epsilon_r + 1)}{2} + \frac{(\epsilon_r - 1)}{2}\left[1 + 12\frac{h}{W}\right]^{-\frac{1}{2}}_{\text{for W/h >1}} \tag{3.4}$$

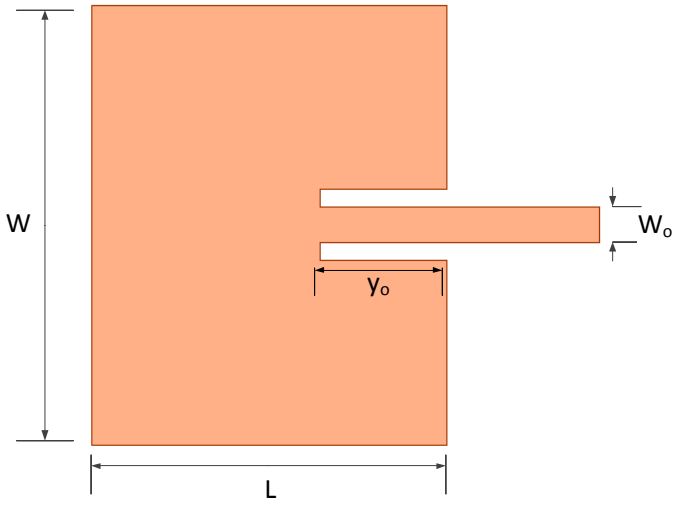

Figure 3.2: A schematic of the patch antenna showing all of its dimensions.

In Figure 3.2, the feed position $y_\circ$ and the width of the transmission line $W_\circ$ can be found using a model presented in [9]. Hence, the antenna parameters were found by solving for equations 3.1 - 3.4 and then using a full wave simulator HFSS to verify the results. Since the above set of equations will result in only an approximate result, one can fine tune the

Antenna Parameter	Value
L	31.8 mm
W	39.3 mm
$y_\circ$	11.3 mm
$W_\circ$	3.18 mm
ϵ_r	3.55
f_r	2.45 GHz

Table 3.1: A summary of the patch antenna parameters.

resonance frequency by slightly varying L and W to arrive at the desired frequency. Table 3.1 summarizes the final results of all the antenna parameters at an operating frequency of 2.45 GHz.

3.2.3 Antenna Fabrication and Measurement

The fabrication process is one of the vital stages learnt during the course of this work. The patch antenna and other structures used in this thesis were fabricated using a T-Tech milling machine available at the University of Waterloo. The fabricated patch antenna, illustrated in Figure 3.3, was etched on an RO4003 Rogers material having a relative permittivity of 3.55.

The return loss of the etched patch was measured using a Vector Network Analyzer (VNA) and, compared to the results obtained from HFSS, the measured return loss is in a good agreement with a slight frequency shift of 0.05 GHz, as shown in Figure 3.4.

3.3 Rectifier Circuit

This section discusses the main components of the rectifier circuit which will be attached to the fabricated antenna to form a full rectenna system. A number of rectifier topologies used in earlier work is reviewed. Furthermore, the input impedance of the agilent Schottky

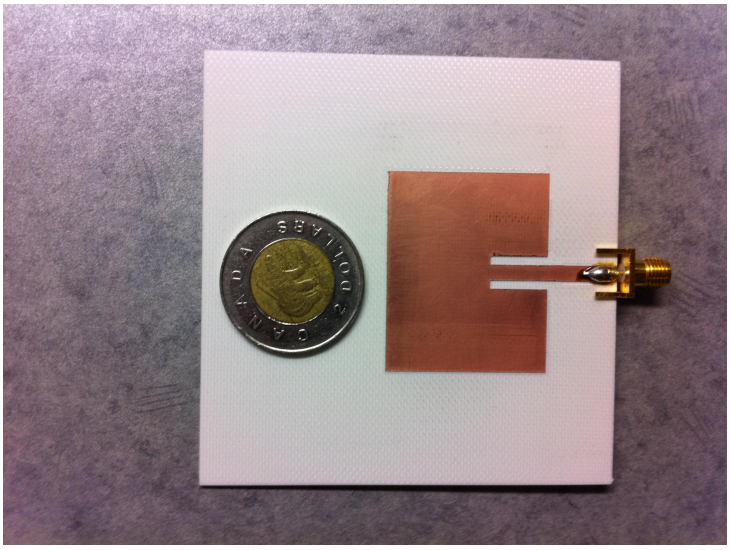

Figure 3.3: The fabricated microstrip-line fed patch antenna.

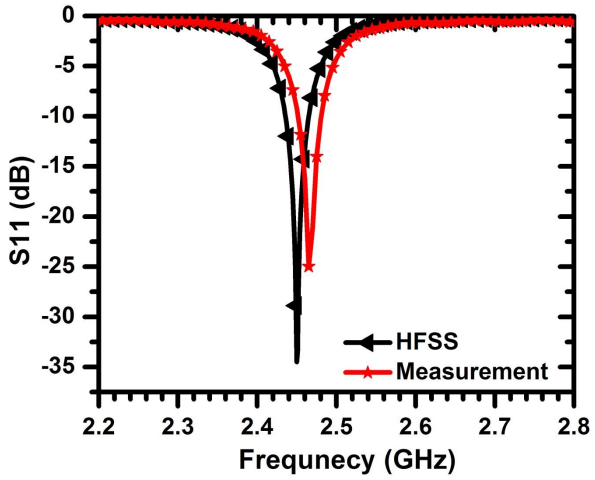

Figure 3.4: Return loss of the fabricated and simulated patch antenna.

diode used is determined using a diode model developed by K. Chang's group. Finally, the designs of the RF and DC filters are presented.

3.3.1 Rectifier Topologies

The main function of the rectifier circuit is to convert AC to DC power using a diode. Different from low frequency rectifiers, microwave rectifiers utilize surface mount diodes that operate at higher frequencies and matching networks to maximize power transfer before and after the diode. Depending on the targeted application, the rectifier circuit can employ a single or dual diodes. The three most common rectifier topologies used in the literature are the series diode, shunt diode, and Villard's voltage doubler rectifier circuits [58]. The series diode rectifier circuit consist of a diode connected in series, a capacitor and a load, as shown in Figure 3.5a. The diode blocks the negative cycle of the captured AC power, then the RC circuit smoothes out the rectified power to obtain a constant output voltage with low ripple. The series diode type of rectifier is ideal for rectennas that use a single feed antenna such as the microstrip-line fed and probe-fed patch antennas because of the simplicity of matching the diode's input impedance to that of the antenna by using a quarter wavelength transformer. The series diode rectifier is commonly used in rectenna applications such as energy harvesting [15] and RFID [55]. Similar to the series type, the shunt diode rectifier circuit consists of a capacitor, a load, and a diode, but with a parallel connection, as illustrated in Figure 3.5b. The shunt diode rectifier has the freedom of using a planar or co-planar microstrip line to link the various rectifier components. This type can usually be found in applications that utilize dual patch antennas, as in [41], or dipole antennas, as in [36]. The Villard's voltage doubler contains dual capacitors, dual diodes and a load, as shown in Figure 3.5c. As the name suggests, the Villard's voltage doubler achieves higher voltage as compared to the single diode type presented above. This can be obtained by using two cascaded diodes that rectify the AC power then, charge the dual capacitors. The Villard's voltage doubler rectifier-circuit was used in [44, 59] for energy scavenging applications.

Here, the series diode rectifier circuit is used since it is the most suitable design for matching the microstrip-line fed patch antenna to the diode. In the following subsections, the type of diode used in the design and the matching networks are discussed.

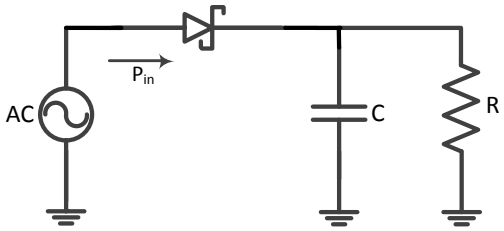

(a) Series-diode rectifier circuit.

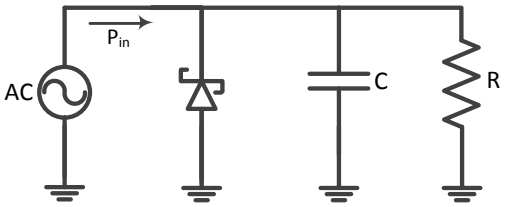

(b) Parallel-diode rectifier circuit.

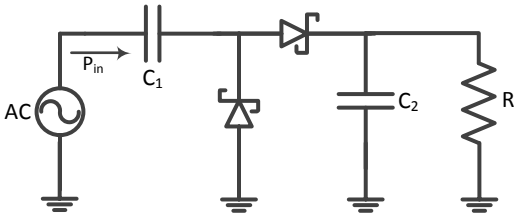

(c) Villard's voltage doubler rectifier circuit.

Figure 3.5: Various rectifier-circuit topologies used in the literature [58].

3.3.2 Schottky Diode

When operating at higher frequencies (*i.e.,* 2.4 GHz), the common P-N junction diode is no longer capable of rectifying the AC signal since it has relatively slower switching capability and higher voltage drop. Instead, a Schottky diode is used to overcome these limitations. Unlike the P-N junction diode, which has a semiconductor-semiconductor junction, the Schottky Barrier Diode (SBD) is formed by plating a metal contact onto an n- or p-type semiconductor [17]. This metal-semiconductor junction acts as a diode, allowing the current to flow in one direction and blocking it in the other. The I-V curve of a Schottky diode is similar to that of a P-N junction diode, with the exception of [47]:

- Faster switching between conducting and non-conducting modes due to the absence of the minority-carrier charge storage effect
- Lower forward voltage drop

The two main classes of Schottky diodes are the n-type and the p-type Schottky diodes. The n-type Schottky diode is formed by a metal and type n semiconductor junction. This type is distinguished by having a high barrier height (indicating low saturation current) and a low series resistance. The n-type Schottky diode is used in applications where a DC bias is accessible, such as mixer and detector applications. The p-type, on the other hand, is made up of a metal and type p semiconductor, and it is characterized by a relatively low barrier height and high series resistance. This type of Schottky diode is used in applications where DC bias is not available, such as square law detector applications [54]. The diode model and proper diode-type selection are presented in the next section.

3.3.3 Diode Model

One of the most important initial steps when designing a rectenna system is determining the input impedance of the Schottky diode. This is due to the non-linear behaviour of the diode as its input impedance depends significantly on the input power level, the load impedance and the frequency of operation. Here, the diode model developed by K. Chang's

group is used due to the promising results and the great agreements between the measured and the simulated results achieved in the literature, as in [50]. For simplicity this model does not take into account the loss due to higher-order harmonics.

The equivalent circuit of a Schottky diode contains a series resistance R_s, a junction resistance R_j, and a junction capacitance C_j as presented in [34]. The load resistance R_L can be varied along with the input power level to arrive at the desired diode input impedance.

The input impedance of the diode Z_d can be found by applying Kirchoff's voltage law to the equivalent circuit of the schottky diode. The final form of the Z_d is given by [34]:

$$Z_d = \frac{\pi R_s}{\cos\theta_{on}\left(\frac{\theta_{on}}{\cos\theta_{on}} - \sin\theta_{on}\right) + j\omega R_s C_j\left(\frac{\pi-\theta_{on}}{\cos\theta_{on}} + \sin\theta_{on}\right)} \tag{3.5}$$

The turn on angle θ_{on} depends on the input power level and can be found from the following relation:

$$\tan\theta_{on} - \theta_{on} = \frac{\pi R_s}{R_L\left(1 + \frac{V_{bi}}{V_\circ}\right)} \tag{3.6}$$

where $V_\circ$ is the output voltage across the load and V_{bi} is the built-in voltage. The junction capacitance C_j is given by:

$$C_j = C_{j\circ}\sqrt{\frac{V_{bi}}{V_{bi} + |V_\circ|}} \tag{3.7}$$

A detailed derivation of Eq. 3.5 can be found in [34].

The Schottky diode selected for the rectenna under test is the Avago's HSMS2860 Schottky diode. This type of diode is optimized to operate at a frequency range of 915 MHz-5.8GHz. The diode has a breakdown voltage V_{br} of 7.0 V and a forward voltage of 0.65 V. The zero bias junction capacitance $C_{j\circ}$ and the series resistance R_s are 0.18 pF and 6.0 Ω, respectively.

A Matlab code, which makes use of the integrated optimization toolbox, is developed to solve for Z_d, θ_{on}, and C_j. Figure 3.6 shows the real part of Z_d, as the load resistance is varied from 1-1000 Ω. Z_d was found to be 170.8 Ω when the load resistance is 250 Ω. Here the choice of the load resistance is kept low to ease the fabrication process as a higher load resistance will lead to a narrower microstrip-line and ,hence, harder to fabricate. The output voltage is usually taken to be 50% of the breakdown voltage to prevent burning the diode, which would create an open circuit. Therefore, the output voltage $V_\circ$ is set at 3.5 V.

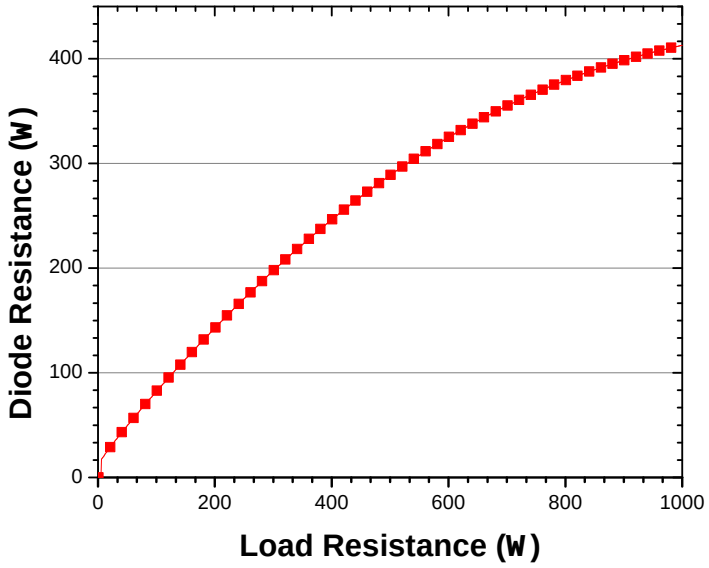

Figure 3.6: Load resistance Vs. Diode input resistance.

3.3.4 RF and DC Filter

At this stage, the two main components of the rectenna system have been designed and analysed and need to be connected through a matching network since they have different input impedances. The primary functions of the pre-rectification or RF filter are to match

the real part of the diode's input impedance to that of the antenna and to prevent higher-order harmonics caused by the non-linear behavior of the diode from radiating by the antenna. A quarter wavelength transformer is inserted between the antenna and the diode to transform the diode resistance to 50 Ω. The impedance of the transformer can be found from the following relation:

$$Z_{QWT} = \sqrt{Z_A Z_d} \tag{3.8}$$

where Z_A is the input impedance of the antenna. Using the diode resistance obtained from Figure 3.6, Z_{QWT} is found to be 92.41 Ω. Hence, using a microstrip-line calculator, the length and width of the quarter wavelength transformer are $l = 16.7\ mm$ and $w = 1.05\ mm$.

Finally, the DC or post-rectification filter is used to tune the reactance of the diode impedance and to prevent any higher frequencies from reaching the load. The DC filter generally consists of a series microstrip line and a shunt capacitor. The Advance Design System (ADS) simulator is used to optimize the capacitor value, and the length and width of the transmission line such that the magnitude of the reflection coefficient (S11) looking from the 50 Ω port into the rectifier circuit is minimized (*i.e.,* a magnitude of $S11 \approx 0$).

From the simulation, it is found that a capacitor value of $C = 56\ pF$ and a transmission line with $l = 40\ mm$ and $w = 1.9\ mm$ would yield maximum matching between the diode and the load.

Figure 3.7 shows the fabricated rectifier circuit with an LED that mimics a load. The rectifier was tested with a high frequency power source; however, the LED did not glow since not enough voltage was developed across it to turn it on.

3.4 Conclusion

The procedures for designing a rectenna system from the antenna to the load were presented. The input impedance of the Agilent diode was determined from a Schottky diode model available in the literature. A quarter wavelength transformer was designed to match

the real part of the diode to that of the antenna. Then, using an ADS simulator, a DC filter was designed to tune out the reactance of the diode impedance. A surface mount LED was used instead of the load as an indicator to test the rectifier circuit. However, the LED did not turn on as the rectifier circuit was not able to deliver enough voltage to the LED. To overcome this issue, some modifications can be made, such as the use of a Villard's voltage doubler circuit for higher voltage levels, and the use of better collector to capture more energy, as will be discussed in the following chapter. Even though the LED did not turn on, the goal for this chapter was achieved since this work is meant to be a preliminary for future work explained in the next chapter.

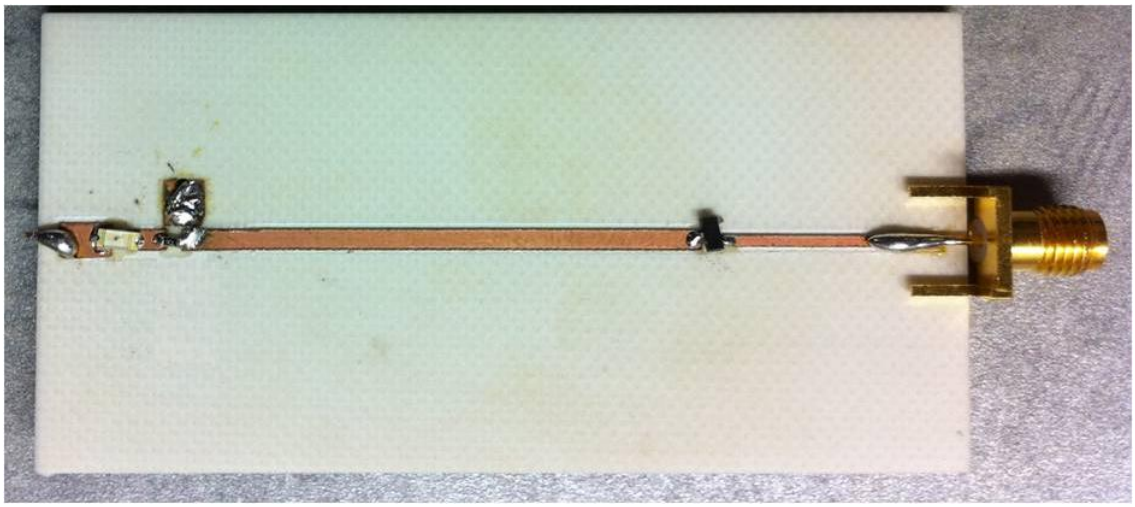

Figure 3.7: Fabricated rectification circuit.

Chapter 4

Electromagnetic Energy Harvesting Using Metamaterial Particles

4.1 Introduction

This chapter presents a novel energy collector based on metamaterial particles in what is known as a Split Ring Resonator (SRR). The subject of metamaterials is briefly introduced, then a feasibility study of SRRs to harvest energy is presented. To prove the concept, a 5.8 GHz SRR is designed and fabricated and then tested using a power source, an Infiniium oscilloscope and a commercially available patch antenna array. In addition, a new efficiency concept is introduced, taking into account the microwave-to-AC conversion efficiency which is missing from earlier work. Finally, a 9X9 SRR array is compared with a 2X2 patch antenna array, both placed in a fixed footprint.

4.2 Metamaterial Background

The emergence of metamaterials has drawn considerable attention from physicists and engineers researching in a wide range of streams. The fact that metamaterials can produce media with negative permittivity and/or permeability has originated numerous or

enhanced existing applications such as creating perfect lenses and absorbers [31, 39], decoupling and modifying antenna characteristics [8, 20, 5], improving the efficiency of solar cells, and detecting cracks [4], to name but a few. Metamaterials can be defined as "artificial media with unusual electromagnetic properties" [49]. Metamaterial particles are formed by assembling electrically small resonators that can take various shapes, geometries and compositions. One of the most common types of resonators is the SRR, which is a metallic inclusion with one or more splits. An SRR can be made of (single or multiple) and (concentric or parallel) electrically small rings. It also can take various shapes, such as those shown in Figure 4.2, or many others analysed in the literature. This work investigates the feasibility of only a single loop resonator to harvest energy, but generalization can be made to any structure available in the literature. When modelling a single-loop SRR (Figure 4.1), it can be realized as a simple LC circuit where the size of the gap (gxw) and the arm length of the metallic ring (L) contribute mainly to the total capacitance and inductance of the structure, respectively. Hence, by varying such dimensions, one can design an SRR to resonate at the desired frequency. A detailed study of the effect of varying the mentioned parameters on the SRR's resonance frequency can be found in [6]. The next section presents a study of the feasibility of such a resonator to harvest electromagnetic energy.

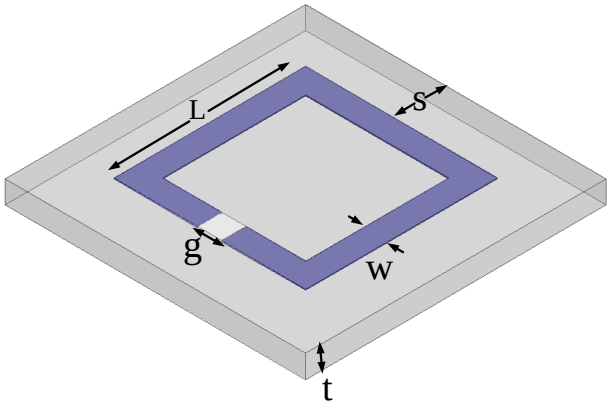

Figure 4.1: Split Ring Resonator unit cell.

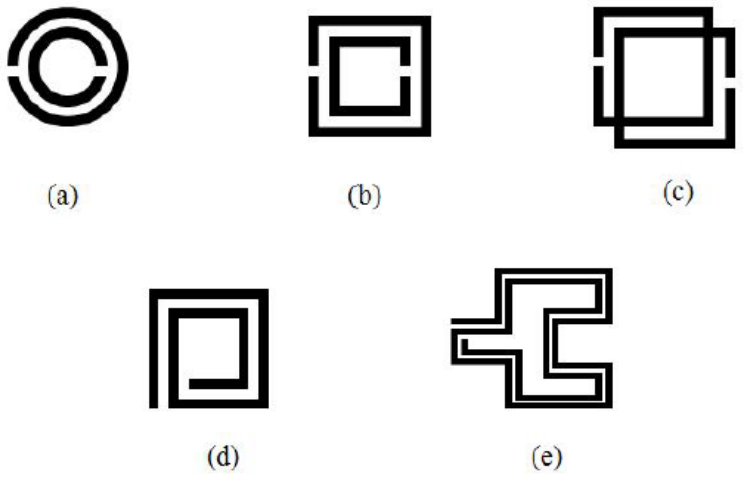

Figure 4.2: Various shapes of metamaterial particles proposed in the literature [7].

4.3 Feasibility of SRRs to Harvest Electromagnetic Energy

When an SRR is excited by a magnetic field normal to its plane, a highly concentrated electric field is developed across the gap of the structure, as indicated by the red color in Figure 4.3. Equally interesting is that the SRR can be excited by an incident magnetic field with various polarizations, as discussed in section 4.5. This concentration of a high electric field is indicative of a build up of high voltage across the gap of the SRR. Hence, this work proposes harvesting this energy by means of a load placed across the gap. To realize this concept using HFSS, a resistive sheet is placed across the gap of an SRR cell, resonating at 5.8 GHz. The designed SRR has dimensions of l =5.9 mm, w = 0.55 mm and g= 0.8 mm. Since the optimal resistance value is not known, the resistive sheet is assigned a variable resistance value ranging between 100 Ω - 10,000 Ω. The SRR is excited by a plane wave such that the H field is perpendicular to the SRR plane. The efficiency of the SRR is then calculated by using the proposed efficiency concept presented in section 4.5. It was found that a single SRR cell has an efficiency of around 40%, with an optimal

resistive load of 2.3 KΩ. This result suggests that the voltage developed across the gap is mostly dissipated by the resistive sheet. Therefore, such SRR structures can potentially be used for harvesting electromagnetic energy.

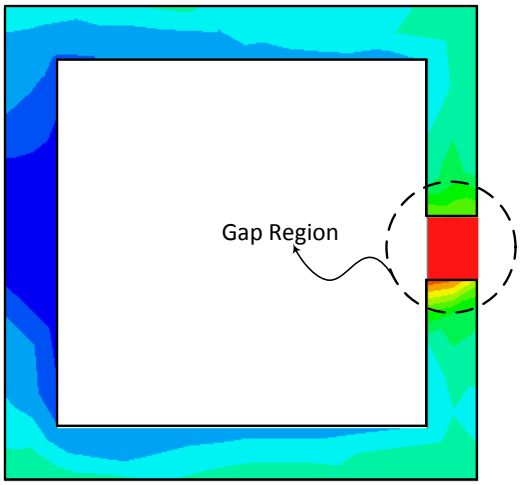

Figure 4.3: Electric field distribution on the plane of the SRR at resonance frequency.

For any radiator to receive energy, it must obey the reciprocity theorem. This theorem states that "in any network composed of linear, bilateral, lumped elements, if one places a constant **current***(voltage)* generator between two **nodes** *(in any branch)* and places a **voltage** *(current)* meter between any other two **nodes** *(in any branch)*, makes observation of the meter reading, then interchanges the locations of the source and the meter, the meter reading will be unchanged" [9]. To ensure that the theorem is not violated, an experiment in HFSS is conducted by designing two radiators, a dipole antenna and a single loop SRR both resonating at the same frequency. The experiment is divided into two cases:

1. A dipole antenna is excited by a current source placed at its feed; then the voltage across the gap of the SRR is recorded (Figure 4.4a).

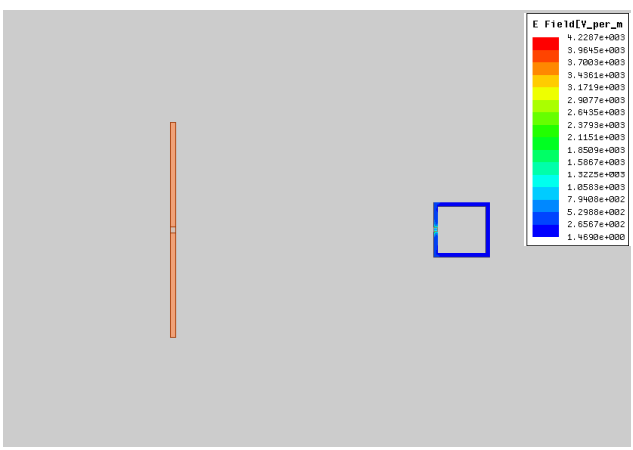

(a) A snapshot of the simulation for case 1.

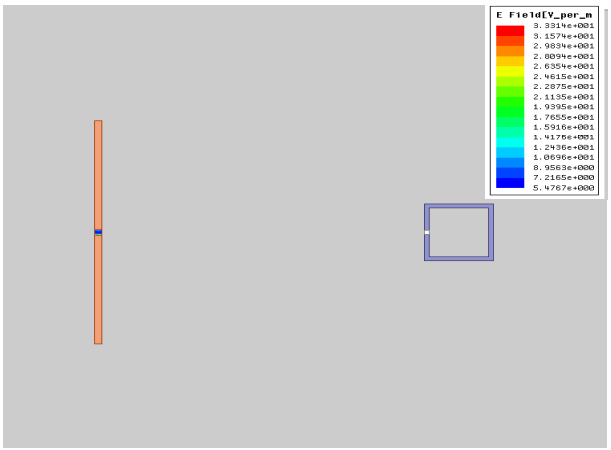

(b) A snapshot of the simulation for case 2.

Figure 4.4: A simulation that verifies the reciprocity therm using a dipole antenna and an SRR.

2. An SRR is excited by a current source placed across its gap; then the voltage across the feed of the dipole antenna is recorded (Figure 4.4b).

The voltage of both cases can be found by

$$V = E \times d \tag{4.1}$$

where E denotes the electric field, and d is the length of the feed (for the dipole) and the length of the gap (for the SRR). Therefore, the voltages for both cases are

$$V_1 = E_1 \times d_1 = (5.988 \times 10^4) \times (0.8 \times 10^3) = \mathbf{47.907\ V}\ \text{for case 1} \tag{4.2}$$

$$V_2 = E_2 \times d_2 = (3.8562 \times 10^4) \times (1.23 \times 10^3) = \mathbf{47.43\ V}\ \text{for case 2} \tag{4.3}$$

It is evident from the voltage values of both cases that the SRR obeys the reciprocity theorem and therefore can be used for collecting electromagnetic energy.

4.4 Proof of Concept

Now, that the simulation analysis has resulted in promising conclusions, the feasibility of using an SRR to harvest electromagnetic energy is validated by testing and measurements. First, the single loop SRR simulated above was fabricated using a Rogers Duroid RT5880 substrate with thickness of 0.79 mm. Then the SRR was loaded with a surface mount resistor of 2.7 KΩ as shown in Fiqure 4.5. Here, the resistor used in the experiment is different from that of the optimal resistor (2.3 KΩ) obtained from the simulation since the latter was not available at the time of the experiment. An experiment was then conducted using the following measurement setup (Figure 4.6):

1. A commercially available 19 dBi gain array antenna operating at 5.8 GHz.
2. An Agilent Infiniium 91304ADSA 12 GHz oscilloscope equipped with a single-ended probe.
3. A high frequency 30 dbm power source.
4. The fabricated single loop SRR.

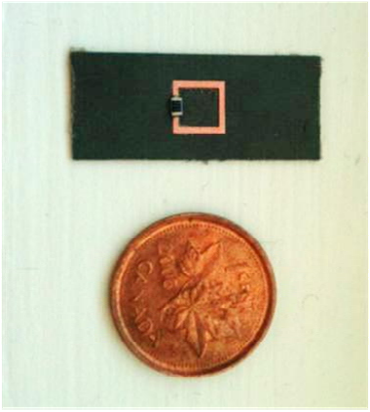

Figure 4.5: Fabricated SRR loaded with a 2.7 KΩ resistor placed at the gap.

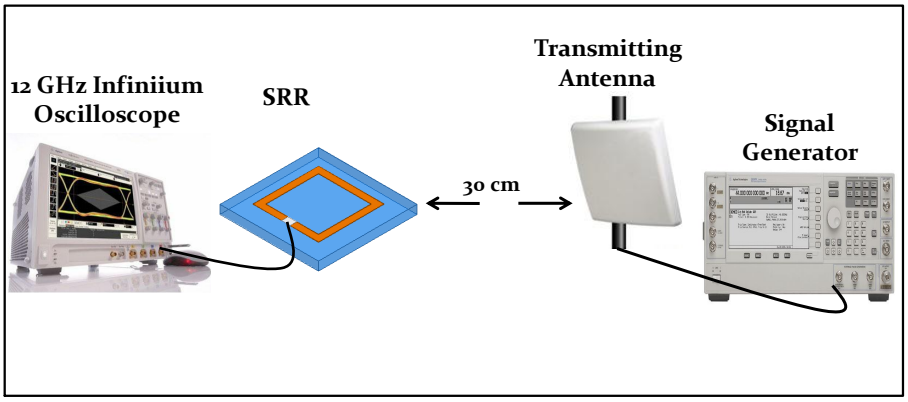

Figure 4.6: Experimental setup.

The SRR was placed 30 cm away from the antenna, and was positioned in such a way that the H-field of the illuminated wave was perpendicular to the plane of the structure. The antenna was excited by a power source with a power level of 24 dbm. Then the voltage across the resistor of the SRR was measured using a single-ended probe of the oscilloscope. A snapshot of the voltage readings (Figure 4.7) shows that the voltage measured across the resistor was 611 mV.

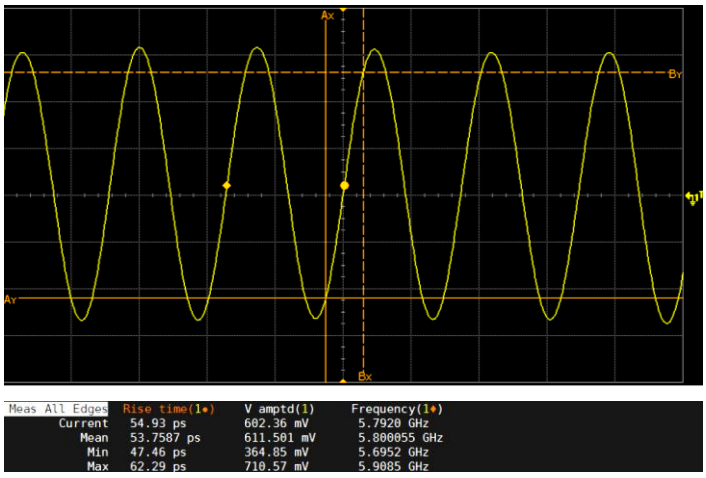

Figure 4.7: A snapshot of the voltage across the gap of the SRR.

4.5 SRR Array Vs. Patch Antenna Array

In this section, a new method for calculating the efficiency of electromagnetic energy collectors such as antennas and SRRs is proposed. Then a comparison in terms of the total microwave-to-AC conversion efficiency between an array of SRRs and an array of antennas placed in the same footprint or area is presented.

As mentioned in Chapter 2, the efficiency of rectenna systems reported in literature does not take into account the microwave-to-AC conversion efficiency of the energy collector. Here, what is meant by microwave-to-AC link is The efficiency of the antenna to convert all the power incident on a specific footprint to available power at its feed position. Therefore, a footprint in square meters must be defined, over which a number of collectors is placed in such a way that the power collected is maximum. Hence the efficiency of a collector as defined above can be found as follows:

$$\eta = \frac{P_{av}}{P_{area}} \tag{4.4}$$

where P_{area} is the total time-average power incident on the footprint, and P_{av} is the the maximum available time-average ac power received by the collector or all collectors occupying the specific footprint under consideration and is available at the feed terminal of the receiving collector. Therefore, P_{av} is given by the following relation:

$$P_{av} = \sum_{i=1}^{n} \frac{V_i^2}{R_i} \tag{4.5}$$

where V_i and R_i are the voltage across and the resistance of collector i. The total number of collectors on a specific footprint is denoted by n.

Considering the efficiency definition just introduced, a demonstration is presented comparing the efficiency of an array of SRRs with an array of patch antennas placed in the same footprint as shown in Figure 4.9. The array of SRRs contained 81 single loops, all of identical size and designed to resonate at around 5.85 GHz. In addition, an array of 2 X 2 identical patch antennas was placed in the same footprint, each resonating at the

same frequency of around 5.85 GHz. The total footprint area was 85 X 85 mm^2. It was reported in the literature that antennas need to be separated by at least $\lambda/2$ to retain their characteristics such as radiation pattern and gain [32]. Therefore, the 4 antennas were separated by a distance of around $\lambda/2$ to ensure maximum power collection by the antennas. In addition, each antenna was fed by a coax probe from beneath. The performance of a probe-fed patch antenna is greatly dependent on the feed position. Hence, the feed position was first analysed by varying the location of the coax with a distance r away from the center of the patch and along the axis that is parallel to the largest dimension of the patch antenna, as shown in Figure 4.9. It was found that the best performance for all of the 4 antennas was achieved when the probe was placed a distance of $r = 2$ mm away from the center of the antenna, as shown in Figure 4.8.

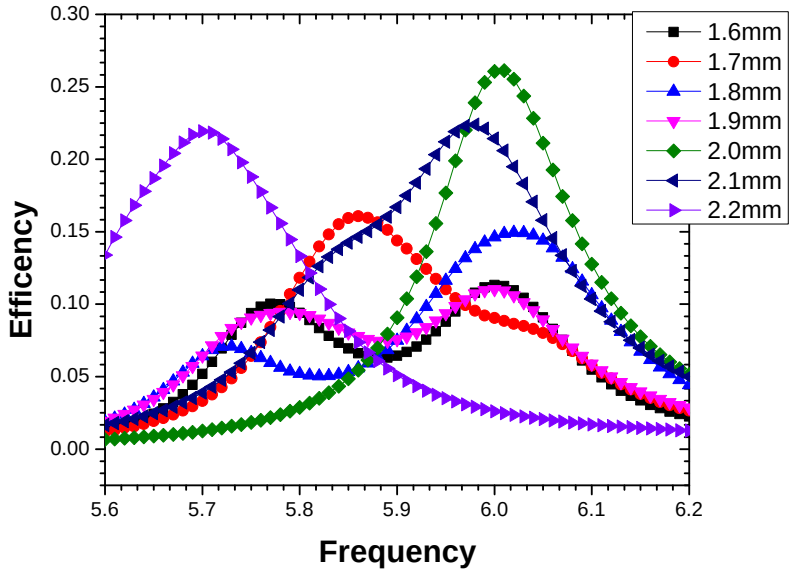

Figure 4.8: The efficiency of the patch antenna with varies coax-probe positions.

In the demonstration, each array was excited by a horn antenna placed a distance of 120 cm away from the array to ensure that the far field condition was satisfied, and a plane wave was incident on the array. Since both the antenna and the SRR are polarized

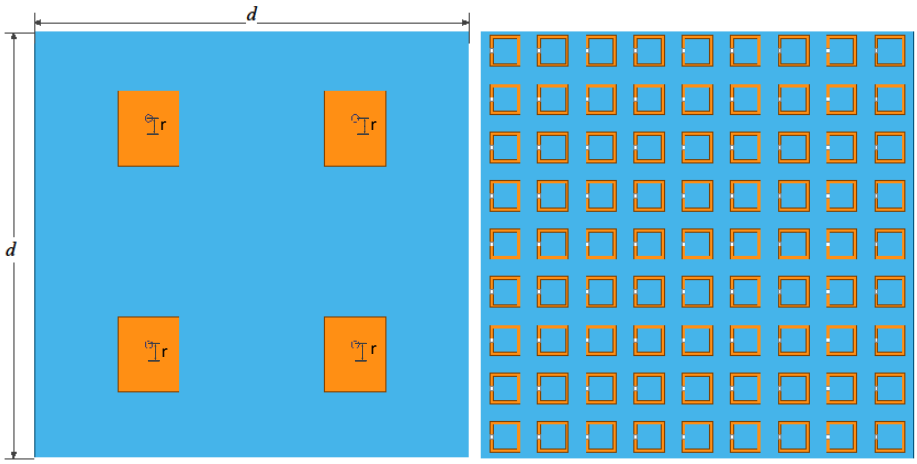

Figure 4.9: a 9 x 9 SRR array and a 2 X 2 patch antenna array occupying the same footprint.

differently, each array was tilted an angle ϕ with respect to an axis normal to the plane of the array, as indicated in Figure 4.10. Three tests were conducted for each array, with angles of 30°, 45°, and 60°. Figures 4.11, 4.12, 4.13 show the efficiency of the antenna array and the SRR array at an angle of $\phi = 30°$, 45° and 60°, respectively.

The following conclusion can be drawn:

- The SRR array resulted in higher efficiency in all three cases.
- The SRR structure is much smaller in size than the antenna in the specific footprint mentioned above, which can contain either 81 SRRs or only 4 patch antennas.
- The bandwidth over which the energy is collected is much wider than that of the antenna array.

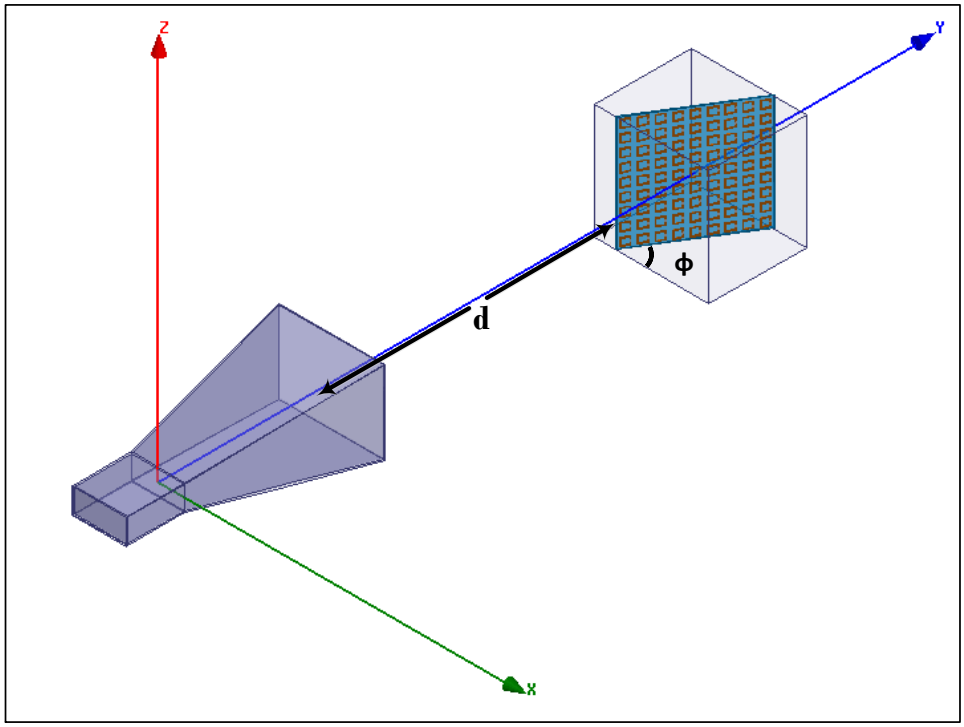

Figure 4.10: Simulation setup for energy harvesting using a horn antenna as the source of radiation and an SRR array as the collector.

4.6 Conclusion

This chapter proposed a new method using SRR cells for collecting electromagnetic energy. The feasibility of using SRRs to harvest microwave energy was studied through simulation by first placing a resistive load across the gap of the single loop SRR, then calculating the power dissipated across the resistor. It was found that around 40 % of the power incident on the single cell SRR is harvested and dissipated by the resistive load. In addition, a simulation experiment was conducted to ensure that the reciprocity theorem is not violated, and the SRR can indeed be regarded as a receiver. An experiment was then conducted to test the feasibility of SRRs to harvest microwave energy. The fabricated SRR cell was excited by an antenna placed 30 cm away, and then the voltage across the gap was measured using a high-frequency oscilloscope. A voltage of 611 mV was observed across the gap when

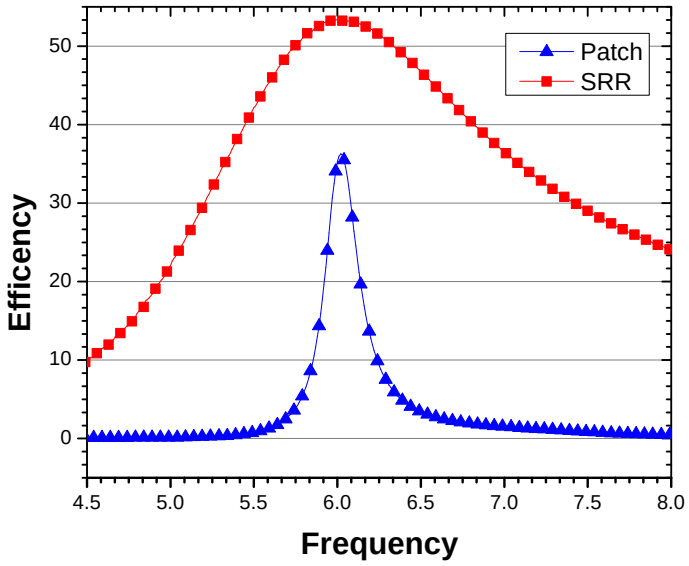

Figure 4.11: Energy harvesting efficiency of the 9 x 9 SRR array Vs. a 2 X 2 patch antenna array both tilted at 30°.

24 dbm power level was pumped into the antenna feed. Finally, the efficiency of an array of SRRs was compared to that of an array of antennas occupying the same footprint. The SRR array resulted in at least 25% more efficiency and a wider energy collection bandwidth than the antenna array.

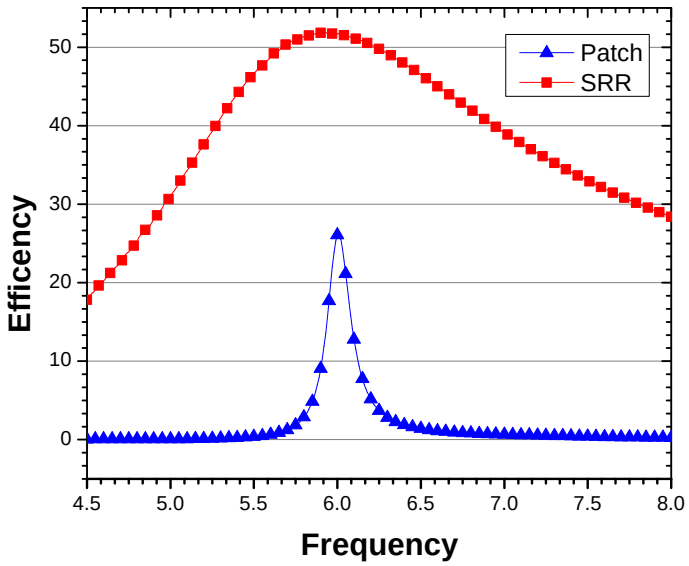

Figure 4.12: Energy harvesting efficiency of the 9 x 9 SRR array Vs. a 2 X 2 patch antenna array both tilted at 45°.

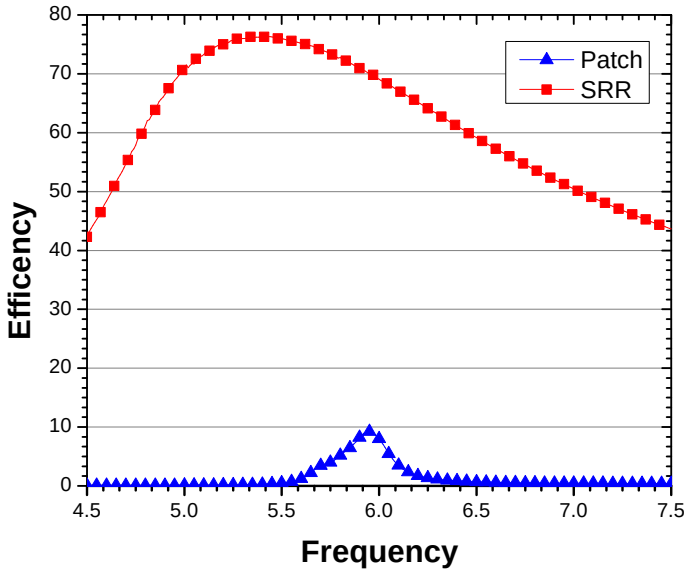

Figure 4.13: Energy harvesting efficiency of the 9 x 9 SRR array Vs. a 2 X 2 patch antenna array both tilted at 60°.

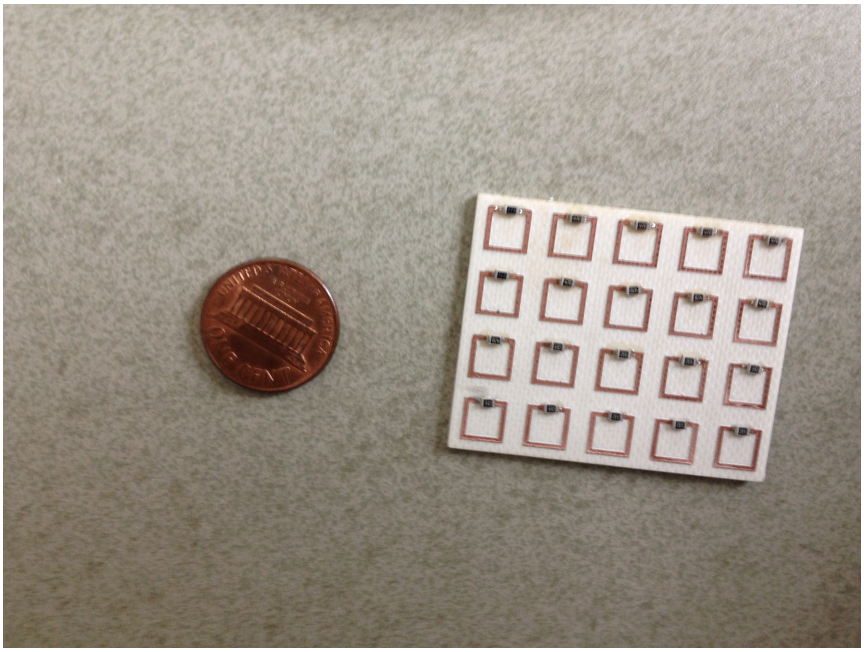

Figure 4.14: A sample of a fabricated 4 X 5 SRR array.

Chapter 5

Conclusion and Future Work

5.1 Conclusion

In this thesis, a review of energy harvesting systems, which in the literature lies under the topic of WPT and rectenna systems, was presented. Then, detailed procedures for designing and fabricating a full rectenna system were provided. A new energy collector based on metamaterial particles was proposed for the purpose of replacing the existing collector (antenna) that has lower efficiency and much larger size than an SRR unit cell. An experiment was conducted both in simulation and in measurements to examine the feasibility of SRRs to harvest microwave energy. The results from both tests show that such metamaterial structure can indeed be used as an energy harvester. Finally, the efficiency of an array of 9 X 9 SRRs was compared to that of an array of 2 X 2 patch antennas placed over an identical area. At least 25% more efficiency and a wider energy collection bandwidth were achieved by the SRR array.

5.2 Future Work

The following suggestions are worth pursuing for future work:

- Improve the design of the rectenna system to provide more output power and hence higher efficiency.
- Investigate the efficiency of various SRR structures such as the those shown in Figure 4.2.
- Study the effect of coupling on the efficiency of both antennas and SRRs.
- Integrate an SRR array, as the one shown in Figure 4.14, to a rectifier circuit for a full Microwave to DC conversion system.

References

[1] Electric light without current. *Literary Digest*, vol.112:30, 1932.

[2] S. Adachi and Y. Sato. Microwave-to-dc conversion loss of rectenna. *Space and Solar Power Review*, 5:357–363, 1985.

[3] A.S.A. Al-Ali, F. Sajwani, A. Al-Muhairi, and E. Shahenn. Assessing the feasibility of using rfid technology in airports. In *RFID Eurasia, 2007 1st Annual*, pages 1–5. IEEE, 2007.

[4] A.M. Albishi, M.S. Boybay, and O.M. Ramahi. Complementary split-ring resonator for crack detection in metallic surfaces. *IEEE MICROWAVE AND WIRELESS COMPONENTS LETTERS*, 22(6), 2012.

[5] H. Attia, L. Yousefi, M.M. Bait-Suwailam, M.S. Boybay, and O.M. Ramahi. Enhanced-gain microstrip antenna using engineered magnetic superstrates. *Antennas and Wireless Propagation Letters, IEEE*, 8:1198–1201, 2009.

[6] K. Aydin, I. Bulu, K. Guven, M. Kafesaki, C.M. Soukoulis, and E. Ozbay. Investigation of magnetic resonances for different split-ring resonator parameters and designs. *New journal of physics*, 7:168, 2005.

[7] M. Bait Suwailam. *Metamaterials for Decoupling Antennas and Electromagnetic Systems*. PhD thesis, University of Waterloo, 2011.

[8] M.M. Bait-Suwailam, M.S. Boybay, and O.M. Ramahi. Electromagnetic coupling reduction in high-profile monopole antennas using single-negative magnetic metama-

terials for mimo applications. *Antennas and Propagation, IEEE Transactions on*, 58(9):2894–2902, 2010.

[9] C.A. Balanis. *Antenna theory: analysis and design*. J. Wiley, 2005.

[10] S.S. Bharj, R. Camisa, S. Grober, F. Wozniak, and E. Pendleton. High efficiency c-band 1000 element rectenna array for microwave powered applications. In *Microwave Symposium Digest, 1992., IEEE MTT-S International*, pages 301–303. IEEE, 1992.

[11] W.C. Brown. Electronic and mechanical improvement of the receiving terminal of a free-space microwave power transmission system. *NASA STI/Recon Technical Report N*, 77:31613, 1977.

[12] W.C. Brown. The history of the development of the rectenna. In *Microwave Power Transmission and Reception*, volume 1, pages 203–212, 1980.

[13] W.C. Brown. The history of power transmission by radio waves. *Microwave Theory and Techniques, IEEE Transactions on*, 32(9):1230–1242, 1984.

[14] WC Brown and JF Triner. Experimental thin-film, etched-circuit rectenna. In *Microwave Symposium Digest, 1982 IEEE MTT-S International*, pages 185–187. IEEE, 1982.

[15] TM Chiam, LC Ong, MF Karim, and YX Guo. 5.8 ghz circularly polarized rectennas using schottky diode and ltc5535 rectifier for rf energy harvesting. In *Microwave Conference, 2009. APMC 2009. Asia Pacific*, pages 32–35. IEEE, 2009.

[16] C.H.K. Chin, Q. Xue, and C.H. Chan. Design of a 5.8-ghz rectenna incorporating a new patch antenna. *Antennas and Wireless Propagation Letters, IEEE*, 4:175–178, 2005.

[17] R. Cory. Schottky diodes. 2009.

[18] J.P. Curty, M. Declercq, C. Dehollain, and N. Joehl. *Design and optimization of passive UHF RFID systems*. Springer Publishing Company, Incorporated, 2010.

[19] RM Dickinson. Evaluation of a microwave high-power reception-conversion array for wireless power transmission. *NASA STI/Recon Technical Report N*, 76:11207, 1975.

[20] S. Enoch, G. Tayeb, P. Sabouroux, N. Guérin, P. Vincent, et al. A metamaterial for directive emission. *Physical Review Letters*, 89(21), 2002.

[21] L.W. Epp, A.R. Khan, H.K. Smith, and R.P. Smith. A compact dual-polarized 8.51-ghz rectenna for high-voltage (50 v) actuator applications. *Microwave Theory and Techniques, IEEE Transactions on*, 48(1):111–120, 2000.

[22] R.B. Erb. Power from space- the tough questions: The 1995 peter e. glaser lecture. *Acta Astronautica*, 38(48):539 – 550, 1996. Benefits of Space for Humanity.

[23] D.G. Fang. *Antenna theory and microstrip antennas*. CRC, 2009.

[24] Y. Fujino, T. Ito, N. Kaya, H. Matsumoto, K. Kawabata, H. Sawada, and T. Onodera. A rectenna for *MILAX*. *Proc. 1st Wireless Power Transmission Conf.*, pages 273–277, 1993.

[25] J. Hansen, C.H. Ahn, and K. Chang. A 5.8 ghz high gain, aperture coupled rectenna utilizing a split ring resonator filter. In *Antennas and Propagation Society International Symposium (APSURSI), 2010 IEEE*, pages 1–4. IEEE, 2010.

[26] P. Hawkes. Anti-collision and transponder selection methods for grouped vicinity cards and pfid tags. In *RFID Technology (Ref. No. 1999/123), IEE Colloquium on*, pages 7–1. IET, 1999.

[27] J. Heikkinen and M. Kivikoski. A novel dual-frequency circularly polarized rectenna. *Antennas and Wireless Propagation Letters, IEEE*, 2:330–333, 2003.

[28] F.J. Huang, C.M. Lee, C.L. Chang, L.K. Chen, T.C. Yo, and C.H. Luo. Rectenna application of miniaturized implantable antenna design for triple-band biotelemetry communication. *Antennas and Propagation, IEEE Transactions on*, (99):1–1, 2011.

[29] S.H. Kim, D.H. Kim, and H.D. Park. Animal situation tracking service using rfid, gps, and sensors. In *Computer and Network Technology (ICCNT), 2010 Second International Conference on*, pages 153–156. IEEE, 2010.

[30] P. Koert, J. Cha, and M. Machina. 35 and 94 ghz rectifying antenna systems. In *SPS 91-Power from Space*, volume 1, pages 541–547, 1991.

[31] NI Landy, S. Sajuyigbe, JJ Mock, DR Smith, and WJ Padilla. Perfect metamaterial absorber. *Physical review letters*, 100(20):207402, 2008.

[32] B.K. Lau and Z. Ying. Antenna design challenges and solutions for compact mimo terminals. 2011.

[33] H. Matsumoto, H. Hirata, Y. Hashino, and N. Shinohara. Theoretical analysis of nonlinear interaction of intense electromagnetic wave and plasma waves in the ionosphere. *Electronics and Communications in Japan (Part III: Fundamental Electronic Science)*, 78(11):104–114, 1995.

[34] J.O. McSpadden. *Rectifying and oscillating integrated antennas*. PhD thesis, Texas A & M University, 1998.

[35] J.O. McSpadden, L. Fan, and K. Chang. A high conversion efficiency 5.8 ghz rectenna. In *Microwave Symposium Digest, 1997., IEEE MTT-S International*, volume 2, pages 547–550. IEEE, 1997.

[36] J.O. McSpadden, L. Fan, and K. Chang. Design and experiments of a high-conversion-efficiency 5.8-ghz rectenna. *Microwave Theory and Techniques, IEEE Transactions on*, 46(12):2053–2060, 1998.

[37] G. Monti, L. Tarricone, and M. Spartano. X-band planar rectenna. *Antennas and Wireless Propagation Letters, IEEE*, 10:1116 –1119, 2011.

[38] K. Nishida, Y. Taniguchi, K. Kawakami, Y. Homma, H. Mizutani, M. Miyazaki, H. Ikematsu, and N. Shinohara. 5.8 ghz high sensitivity rectenna array. In *Microwave Workshop Series on Innovative Wireless Power Transmission: Technologies, Systems, and Applications (IMWS), 2011 IEEE MTT-S International*, pages 19–22. IEEE, 2011.

[39] J.B. Pendry. Negative refraction makes a perfect lens. *Physical Review Letters*, 85(18):3966–3969, 2000.

[40] Y.J. Ren. *Microwave and millimeter-wave rectifying circuit arrays and ultra-wideband antennas for wireless power transmission and communications*. PhD thesis, TEXAS A&M UNIVERSITY, 2007.

[41] Y.J. Ren and K. Chang. 5.8-ghz circularly polarized dual-diode rectenna and rectenna array for microwave power transmission. *Microwave Theory and Techniques, IEEE Transactions on*, 54(4):1495–1502, 2006.

[42] Y.J. Ren, M.F. Farooqui, and K. Chang. A compact dual-frequency rectifying antenna with high-orders harmonic-rejection. *Antennas and Propagation, IEEE Transactions on*, 55(7):2110–2113, 2007.

[43] Y.J. Ren, M.Y. Li, and K. Chang. 35 ghz rectifying antenna for wireless power transmission. *Electronics Letters*, 43(11):602–603, 2007.

[44] T. Salter, G. Metze, and N. Goldsman. Application of a parasitic aware model to optimize an rf energy scavenging circuit fabricated in 130 nm cmos. In *Recent Advances in Microwave Theory and Applications, 2008. MICROWAVE 2008. International Conference on*, pages 303–305. IEEE, 2008.

[45] T.K. Sarkar. *History of wireless*, volume 177. Wiley-IEEE Press, 2006.

[46] J. Schlesak, A. , Alden, and T. Ohno. *SHARP* rectenna and low altitude flight trials. *Global Telecommunications , IEEE Conf.*, 1985.

[47] A.S. Sedra and K.C. Smith. *Microelectronic circuits*, volume 1. Oxford University Press, USA, 1998.

[48] K.M.Z. Shams and M. Ali. Wireless power transmission to a buried sensor in concrete. *Sensors Journal, IEEE*, 7(12):1573–1577, 2007.

[49] L. Solymar and E. Shamonina. *Waves in metamaterials*. Oxford University Press, USA, 2009.

[50] B. Strassner and K. Chang. 5.8-ghz circularly polarized rectifying antenna for wireless microwave power transmission. *Microwave Theory and Techniques, IEEE Transactions on*, 50(8):1870–1876, 2002.

[51] B. Strassner and K. Chang. Passive 5.8-ghz radio-frequency identification tag for monitoring oil drill pipe. *Microwave Theory and Techniques, IEEE Transactions on*, 51(2):356–363, 2003.

[52] B.H. Strassner II and K. Chang. Rectifying antennas (rectennas). *Encyclopedia of RF and Microwave Engineering*, 2005.

[53] Y.H. Suh and K. Chang. A high-efficiency dual-frequency rectenna for 2.45-and 5.8-ghz wireless power transmission. *Microwave Theory and Techniques, IEEE Transactions on*, 50(7):1784–1789, 2002.

[54] Avago Tech. Application note 1088, avago tech. 2010.

[55] Y. Tikhov, I.J. Song, and Y.H. Min. Rectenna design for passive rfid transponders. In *Wireless Technologies, 2007 European Conference on*, pages 237–240. IEEE, 2007.

[56] IH White, MJ Crisp, and RV Penty. A photonics based intelligent airport surveillance and tracking system. In *Advanced Information Networking and Applications (AINA), 2010 24th IEEE International Conference on*, pages 11–16. IEEE, 2010.

[57] H. Yagi and S. Uda. On the feasibility of power transmission by electric waves. *in Proceedings of the Third Pan-Pacific Science Congress*, vol.2:1305–1313, 1926.

[58] W.S. Yeoh. *Wireless Power Transmission (WPT) Application at 2.4 GHz in Common Network*. PhD thesis, RMIT University, 2010.

[59] T.C. Yo, C.M. Lee, C.M. Hsu, and C.H. Luo. Compact circularly polarized rectenna with unbalanced circular slots. *Antennas and Propagation, IEEE Transactions on*, 56(3):882–886, 2008.

[60] T.W. Yoo and K. Chang. Theoretical and experimental development of 10 and 35 ghz rectennas. *Microwave Theory and Techniques, IEEE Transactions on*, 40(6):1259–1266, 1992.

[61] N. Zhu and R.W. Ziolkowski. Metamaterial-inspired, near-field resonant parasitic gps antennas: Designs and experiments. In *Antennas and Propagation (APSURSI), 2011 IEEE International Symposium on*, pages 658–660. IEEE, 2011.

[62] N. Zhu, R.W. Ziolkowski, and H. Xin. A metamaterial-inspired, electrically small rectenna for high-efficiency, low power harvesting and scavenging at the global positioning system l1 frequency. *Applied Physics Letters*, 99:114101, 2011.